AAPT PHYSICS EDUCATION | AMERICAN JOURNAL of PHYSICS

A simple laser cooling and trapping apparatus for undergraduate laboratories

Angela S. Mellish and Andrew C. Wilson

Citation: Am. J. Phys. **70**, 965 (2002); doi: 10.1119/1.1477435
View online: http://dx.doi.org/10.1119/1.1477435
View Table of Contents: http://ajp.aapt.org/resource/1/AJPIAS/v70/i9
Published by the American Association of Physics Teachers

APPARATUS AND DEMONSTRATION NOTES

Jeffrey S. Dunham, *Editor*
Department of Physics, Middlebury College, Middlebury, Vermont 05753

This department welcomes brief communications reporting new demonstrations, laboratory equipment, techniques, or materials of interest to teachers of physics. Notes on new applications of older apparatus, measurements supplementing data supplied by manufacturers, information which, while not new, is not generally known, procurement information, and news about apparatus under development may be suitable for publication in this section. Neither the *American Journal of Physics* nor the Editors assume responsibility for the correctness of the information presented. Submit materials to Jeffrey S. Dunham, *Editor.*

A simple laser cooling and trapping apparatus for undergraduate laboratories

Angela S. Mellish and Andrew C. Wilson
Physics Department, University of Otago, P.O. Box 56, Dunedin, New Zealand

(Received 26 November 2001; accepted 18 March 2002)

We present detailed instructions for the construction of a pyramidal-style laser cooling and trapping apparatus. This scheme requires only a single beam, rather than the three pairs of orthogonal beams of the standard magneto-optical trap, which greatly simplifies the geometry and substantially reduces the cost. The trap is based largely on low-cost commercially available items and is simple to construct. It is remarkably insensitive to alignment and reliable to operate. Using a single laser beam with an intensity of 1.3 mW/cm^2 we cool and trap more than 4 million rubidium atoms.

[DOI: 10.1119/1.1477435]

I. INTRODUCTION

Laser cooling and trapping has become a common feature in physics research laboratories world-wide. The ''workhorse'' in this field is the magneto-optical trap (MOT),[1] which has played a key role in the production of Bose–Einstein condensates.[2] It has also been used extensively to perform experiments in atom optics. The new regime of ultralow temperature provides researchers with precise control over the motion of atoms and has led to important applications, such as the atom laser.[3] The rapid development of the field, the elegant descriptions of behavior provided by the researchers,[4] and the awarding of Nobel prizes,[5] have all generated tremendous interest among physics students. More recently, this interest has been fueled by dramatic demonstrations with Bose–Einstein condensates, including such phenomena as interference fringes,[6] nonlinear optics[7] with matter waves, and collapsing and exploding condensates.[8] Laser cooling and trapping involves many undergraduate physics course topics, such as quantum mechanics, condensed matter, thermodynamics and statistical mechanics, atomic physics, optics and electromagnetism. In addition, when the technology is used in an undergraduate laboratory it provides an excellent introduction to lasers, ultrahigh vacuum, electronics, magnetic fields, light polarization, imaging systems, and photodetection.

In 1995, Wieman *et al.* provided a ''recipe'' for the construction and operation of an inexpensive apparatus for laser cooling and trapping of rubidium atoms, that is ideally suited for development and use in an undergraduate laboratory.[9] The article is important because its instructive style gives undergraduate students access to an exciting frontier in quantum physics. Their most useful innovation is a simple but effective low-pressure vapor cell. In addition to a wealth of practical advice that builds on a previous paper on an external cavity diode laser design,[10] the article provides an excellent introduction to the physics of laser cooling and trapping. Since this work, a number of authors have published related material in a similar style.[11–14]

In this paper we describe the construction of a simplified laser cooling and trapping apparatus based on a pyramidal mirror configuration developed by Lee *et al.*[15] This scheme requires only a single beam rather than the three pairs of orthogonal beams of the standard MOT. Although simple to construct and trivial to align, this MOT scheme has proved its usefulness in research labs where it has been used to produce dense slow atomic beams with cesium[16] and potassium atoms.[17] We describe an optical system that is an alternative to that described in Ref. 9, and which greatly simplifies the geometry and substantially reduces the cost. The trap is based largely on low-cost commercially available items. It is simple to construct and remarkably insensitive to alignment. In a similar style to the previous article by Wieman *et al.*, a step-by-step ''recipe'' is given for the construction and operation of the pyramidal trap. The optical and vapor cell configuration described here replaces that described in Ref. 9: we use a similar laser setup, no new optical components (with the exception of a pyramidal mirror), and similar vacuum equipment. Where features of our apparatus are common to that described by Wieman *et al.* we generally refer the reader to Ref. 9. The purpose of this note is to provide useful alternatives to some key components of Ref.

9, and therefore we avoid repeating some of the discussion and all of the background material presented in the previous work.

Section II provides details on external cavity diode laser frequency stabilization and tuning; Sec. III covers the optical system including the pyramidal mirror; Sec. IV describes the vacuum chamber and its assembly; Sec. V discusses magnetic fields; and Sec. VI outlines operation of the trap, presents measurements, and discusses features specific to the pyramidal MOT. A list of components used is given in the Appendix.

II. LASER STABILIZATION AND TUNING

As outlined in Ref. 9, laser cooling and trapping of ^{87}Rb atoms is usually performed with two 780-nm external cavity diode lasers (ECDLs): a trapping laser tuned slightly below the $5S_{1/2}F=2\rightarrow 5P_{3/2}F'=3$ transition, and a hyperfine pumping (or repumping) laser tuned to the $5S_{1/2}F=1 \rightarrow 5P_{3/2}F'=2$ transition. A simple and effective design for these lasers is given in Ref. 10, and other popular designs are given in Refs. 18 and 19. The design by Arnold *et al.* requires almost no special machining (since it is based on commercially available components) and the alignment is easy and robust. Any of these external cavity diode laser designs is suitable for our purpose. As an alternative to having two ECDLs, Feng *et al.* have published designs for frequency modulating a single ECDL to produce an output with frequency components at both the trapping and repumping frequencies.[11] In this case the laser injection current is modulated at half the ground state hyperfine splitting ($\frac{1}{2}\times 6.835$ GHz), so that a frequency sideband is tuned to each of the two transitions.

Saturated absorption spectrometers for each laser reveal the rubidium hyperfine structure, and servo-control circuitry is used to stabilize the laser frequencies with respect to this structure. Reference 9 describes the standard optical layout for saturated absorption spectroscopy; however, an alternative to this is simply to retro-reflect a beam through a vapor cell,[20] as shown in Fig. 1.

This scheme is trivial to align and produces distinct hyperfine peaks on the Doppler-broadened absorption signal, although care must be taken to avoid directing the beam back to the ECDL as this leads to severe laser frequency instability (the early indicator of which is ''ripples'' on the saturated absorption spectrum).

There are two common schemes for servo-controlling the laser frequency. In one scheme (described fully in Ref. 9), the laser is tuned to the side of a resonance peak and an error signal is generated by comparing the saturated absorption photodiode signal at this frequency with a stable reference voltage. The advantage of this scheme is that it is simple, but a drawback for some applications is that the laser cannot be locked on resonance (as is desirable for the hyperfine pumping laser). In the other scheme, the laser frequency is dithered (i.e., weakly modulated compared to the transition linewidth) and an error signal is derived using phase-sensitive detection (PSD). The advantage of this scheme is that the laser is locked to the hyperfine peak, and therefore its frequency is well-known. In each case the error signal is sent to an integrator before being fed back to the laser. Low speed (typically less than a few kHz) feedback can be directed to the ECDL's piezoelectric tuning element; however, improved performance can be achieved using higher frequency dither (100 kHz is common in our laboratory) and a double integrator that produces a high speed error signal for feedback to the laser diode injection current and a low speed error signal for the piezo. In this work we use the latter scheme with an inexpensive MiniCircuits mixer [1] for PSD (rather than an expensive lock-in amplifier) and the double integrator described by Rovera *et al.*[20] The high speed integrator output is fed directly to the modulation input of a laser current controller described in Ref. 21.

To tune the trapping laser frequency to the desired one to three linewidths (or 6–18 MHz) below resonance, a dc magnetic bias field is applied to the saturated absorption vapor cell in order to Zeeman shift the hyperfine level. By circularly polarizing the incident saturated absorption beam (using a $\lambda/4$ plate between the beamsplitter and vapor cell, as shown in Fig. 1), atoms are pumped into either of the $F=2$, $m_F=\pm 2$ states, for which the tuning with a uniform magnetic field is ± 1.4 MHz/G (or ± 14 GHz/T). However, the coil wound around our vapor cell is approximately the same length as the glass cell, so the field is not uniform along the axis (the field decreases sharply at the ends of the coil). The range of magnetic field values gives rise to a broadening of the hyperfine transitions, in addition to a Zeeman shift of the peak that corresponds to the average value of the magnetic field within the cell. Our coil requires a slightly greater current than would be needed for a longer solenoid, but the convenience of using a short coil is considerable. Our reference cell coil has 170 turns, a diameter of 28 mm, and a length of 150 mm, providing a tuning of 16.1 MHz/A (confirmed by making a beat measurement with a second laser locked to a hyperfine peak). The tuning range using this method is greater than for the simple side-locking scheme.

III. OPTICAL SYSTEM AND PYRAMIDAL MIRROR CONSTRUCTION

A diagram of the optical layout (excluding details of the two ECDLs and saturated absorption setups) is shown in Fig. 2. The entire optical setup and vacuum chamber fits onto a $0.6\ \text{m}\times 0.6\ \text{m}$ optical breadboard [2]. Unlike the standard six-beam MOT, the pyramidal MOT requires only one large beam and a single $\lambda/4$ waveplate [3] (not six), and this makes optical alignment trivial and reduces the cost substantially. The trapping and pumping lasers each produce an output of approximately 20 mW. A small fraction of each laser output (approximately 10%) is split off, using glass plates, for saturated absorption as described in Sec. II. The pumping beam is expanded and made circular in its cross-section using an $f=20$-mm spherical lens and an $f=25$-mm cylindrical lens [4], to a diameter of 20 mm at the pyramid. The shape of the trapping beam is made circular using an anamorphic prism pair [5]: it is then reflected from mirror M2 (for guiding into the pyramid), and circularly polarized using a 10-mm-diam multiple order $\lambda/4$ plate [3]. Before entering the pyramidal mirror it is expanded to a diameter of approximately 30 mm using a pair of singlet lenses ($f=20$ and 520 mm) [4] that are spaced by the sum of their focal lengths in a simple telescope configuration.

The pyramidal mirror consists of four silver-coated mirrors [6] glued in a stainless steel mount which ensures that the angle between opposing pairs of mirrors is 90°. The shape of the reflective surface of each mirror is shown in Fig. 3(a). Each mirror forms an isosceles triangle with a side-length ratio of $1:\frac{\sqrt{3}}{2}:\frac{\sqrt{3}}{2}$ and a vertex angle of 70.5° with two

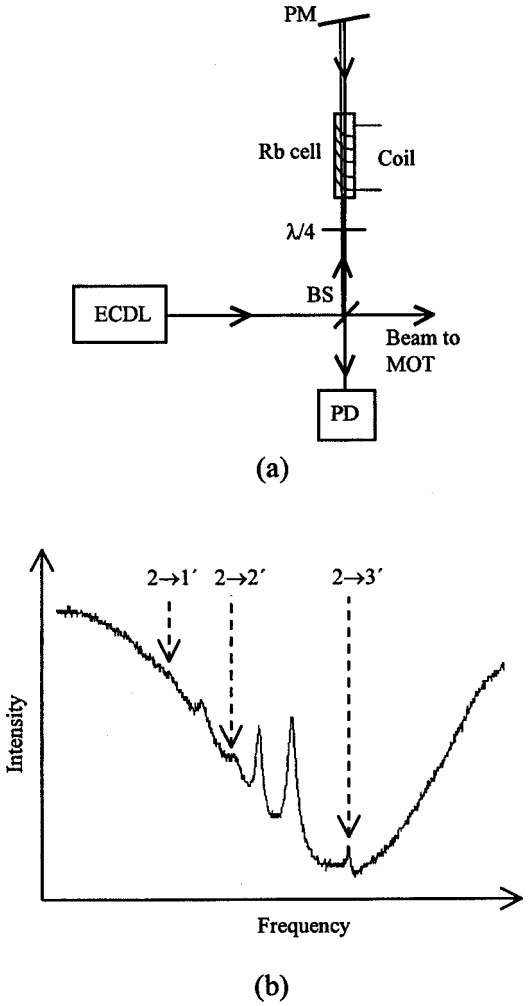

Fig. 1. (a) Simple saturated absorption configuration. PD—photodiode; BS—beamsplitter; PM—partial mirror. The coil and λ/4 waveplate are used for tuning the trapping laser only, and are not present in the saturated absorption setup for the pumping laser. (b) Typical saturated absorption spectrum for $F=2$ ground state of ^{87}Rb. The frequency spacing between the $F=2$ to $F'=1$ and the $F=2$ to $F'=3$ transitions is 424 MHz, and the unlabeled peaks are crossover transitions.

corners altered as shown by the dotted lines in the figure. This shape was chosen to alter the shape of the pyramid base for easy installation into the cylindrical vacuum chamber. The edges of the mirrors along the sides of equal length are bevelled at 30° so that they can be assembled to form a hollow pyramid with minimal gaps between the reflective mirror surfaces. The mirrors are mounted in a 109° cone that was machined into a stainless steel block and then held in place with a small amount of Torr Seal ultrahigh vacuum epoxy [7]. Details on how to prepare and mount the mirrors for ultrahigh vacuum are given in Sec. IV.

The mirror substrates were constructed in-house using standard glass cutting and grinding equipment, although there are many optics companies which offer such services [6]. The substrates are 2-mm-thick float glass. These are cut to the approximate shape shown in Fig. 3(a) using a diamond saw, then each is attached (using a thin layer of black wax) to the end of a specially shaped brass rod for grinding to the required shape. The four brass rods are each made using rod stock of square cross-section: one altered to form a pentagonal cross-section [as shown in Fig. 3(c)] and an end is cut precisely at a 45° diagonal. When placed together the rods form a hollow pyramid with an octagonal base. The edges of the substrate are now ground until they are parallel to the sides of the brass rod. This simple method ensures the correct angle for the vertex of each mirror and provides all the appropriately bevelled edges. We estimate the error in the 90° angle between any two opposing mirrors to be less than 2°, but as we discuss in Sec. VI this alignment is not critical. The substrates are then coated with silver to give a reflectivity of approximately 97% at 780 nm. A silver coating was chosen because it has a higher reflectivity than aluminum at 780 nm, is more robust than gold, and is less likely to cause unwanted changes to the polarization than a typical dielectric coating. This last feature is important for the pyramidal MOT, although Arlt *et al.* have designed a dielectric mirror coating which specifically addresses this issue and has a higher reflectivity than silver.[16] Measurements on our silver coating gave $R_s=97\%$, $R_p=96\%$, and the contamination of circularly polarized light with the wrong handedness after one reflection is 2.5%.

IV. TRAPPING CELL AND CONSTRUCTION

The hollow pyramidal mirror is mounted in an ultrahigh vacuum chamber consisting of a stainless steel four-way reducing cross [8] with Conflat-type flanges sealed with copper gaskets. Attached to the cross are a 2-l/s ion pump [9] on an intermediate piece extension tube [10], a high current feedthrough [11] connecting to a rubidium source [12] within the chamber, a glass-to-metal connection [13] to a turbomolecular pump, and a viewport [14] in front of the pyramidal mirror. A schematic of the vacuum chamber is shown in Fig. 4. These components are standard items available from many vacuum component suppliers. Low vapor pressure epoxy is used to locate the pyramid within the chamber, but not to seal the chamber, so that baking is extremely unlikely to cause a vacuum leak.

Before gluing, the mirrors and mount are cleaned by rinsing in distilled water, dichloromethane, and finally acetone (analytical reagent quality) [15]. The stainless steel mount is cleaned using an ultrasonic bath, but the mirror coatings are extremely fragile and are not touched (even with optical cleaning tissue). Once cleaned, the components are handled only with clean optical tissue to position and glue the mirrors into the mount. Care is taken with the epoxy to avoid trapping gas in the space between the back surfaces of the mirror and the conical mount. To improve the conductance to this region, a 5-mm-diam hole is drilled through the steel block at the vertex of the hollow cone. The Torr Seal epoxy takes approximately 24 h to cure: and during this period the pyramid is kept in a clean dry place. Once the mirrors have been mounted, the hollow pyramid is then installed into the tubular vacuum chamber.

The square cross-section of the stainless steel mounting block is chosen so that when the pyramid is placed into the horizontal tubular chamber it rests on two edges of the mounting block. The pyramid is held in place with a small amount of epoxy. In our case, the inner diameter of the vacuum tube is 34 mm, and the sides of the square base of the stainless steel mounting block are 23 mm long. Minimizing how far the pyramid is slid into the vacuum tube maximizes the range of angles over which the MOT can be viewed, but a spacing between the base of the pyramid and

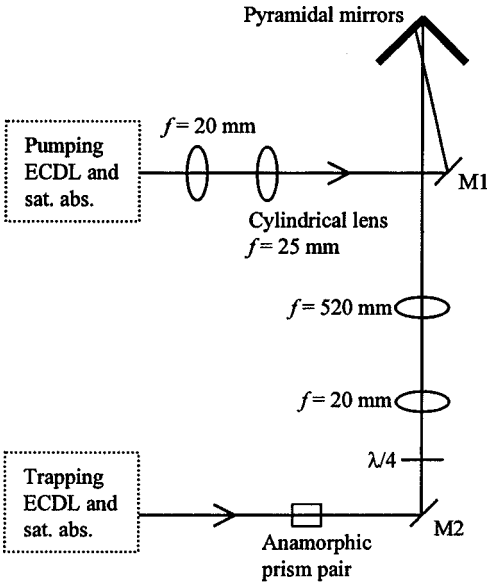

Fig. 2. Diagram of the optical layout for the pyramidal trap.

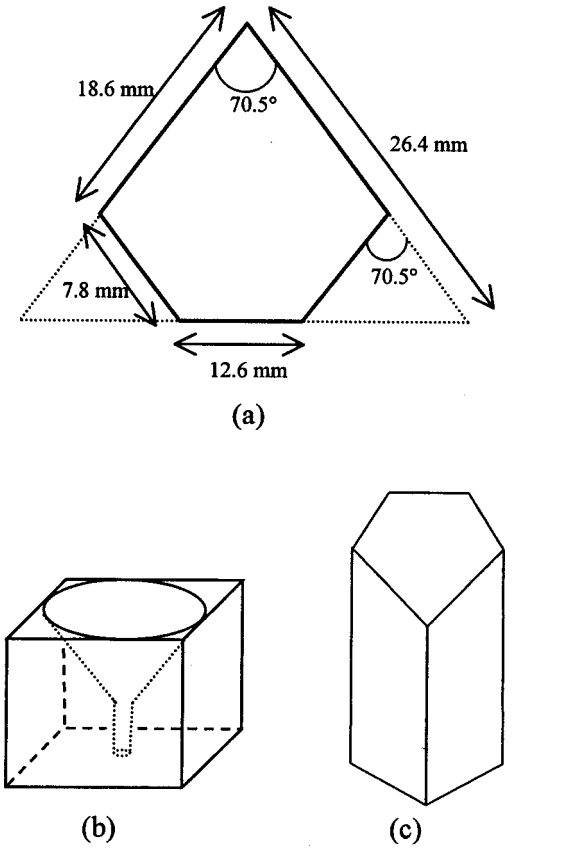

Fig. 3. (a) Shape of the reflective surface of each of the four mirrors forming the hollow pyramid. (b) Stainless steel mounting block for the pyramidal mirror. (c) Brass rod to which each substrate is attached for precise shaping.

the internal surface of the viewport is needed to allow rubidium to diffuse into the hollow pyramid region. We found that a spacing of 16 mm works well.

The rubidium source we use is the same type as that described in Ref. 9. These rubidium dispensers are attached to the high current feedthrough using screw-type connectors that were supplied with the feedthrough.

In our setup, the vacuum chamber is attached to a turbomolecular pump via a glass-to-metal adapter. The turbo pump evacuates the chamber to a pressure of around 10^{-7} Pa before the small ion pump is switched on: the turbo pump is then removed by pinching off the glass connection tube. Although not convenient for multiple pumping and venting cycles, the sealing off of glassware is cheaper than purchasing an all-metal valve rated to 10^{-7} Pa.

For advice on assembling ultrahigh vacuum components,[22] one should refer to supplier instructions or a reference such as Ref. 23. Once all of the flanges on the vacuum chamber have been tightened, and the glassware connection to the turbo pump is made (by a glassblower), the turbo pump is switched on. A quick leak-check of the flanges can be made by monitoring the pressure while squirting acetone on the gaskets. If there is a leak, the pressure may drop briefly as the acetone blocks the hole, but it then increases rapidly as the acetone vaporizes upon entering the vacuum.

To accelerate the pumping process, it is important to bake the vacuum system. To extend the lifetime of our 2-l/s ion pump, we bake the chamber only while pumping with the turbomolecular pump: we switch on the ion pump after baking, once the pressure is low (10^{-7} Pa). In our case, the maximum baking temperature is limited to approximately 390 K by the epoxy, but this is adequate for removing water, which is the dominant contaminant with new vacuum components. We wrap each of the flanges in aluminum foil in order to keep a uniform temperature, and then enclose the entire vacuum chamber along with a 1-W infrared heater element (controlled by a variac) in a few layers of aluminum foil, in a type of make-shift oven. While pumping with the turbo pump, we then heat the entire vacuum chamber, including the glass-to-metal adapter, to a temperature of 370 K for 48 h. The change in temperature is made slowly (over a period of 4 h) to avoid leaks induced by thermal gradient induced stress.

After this bakeout period, but before the ion pump is switched on, it is important to degas the rubidium dispensers by applying the operating current to each. When this is done for the first time the pressure increases substantially, and it is necessary to increase the current slowly to protect vacuum gauges and the pump (although this is unlikely to be a problem for a turbo pump). When the dispenser is fully degassed, the pressure on a gauge near the turbo pump does not increase, because essentially only rubidium is released and in a freshly baked system the metal vapor adheres to the chamber walls.

Once the dispenser has been degassed and the pressure has decreased to the postbake value (or close to this), the ion pump is switched on. When this is done for the first time, the discharge in the ion pump causes significant outgassing. To extend the lifetime of the small ion pump, we keep the turbo pump attached, so as to assist with removing this gas load. After degassing the ion pump, the turbo pump is detached by pinching off the glass connection tube. The pinching off process also releases gas, but the pressure slowly decreases until the ion pump current (a crude measure of pressure) is immeasurably small after a period varying from 2 to 12 h (depending on the history of the vacuum chamber and pump), indicating a pressure below 10^{-7} Pa. If the ion pump current does not decrease sufficiently, the ion pump leakage current should be checked (by removing the ion pump magnet) before assuming that the pressure is too high.

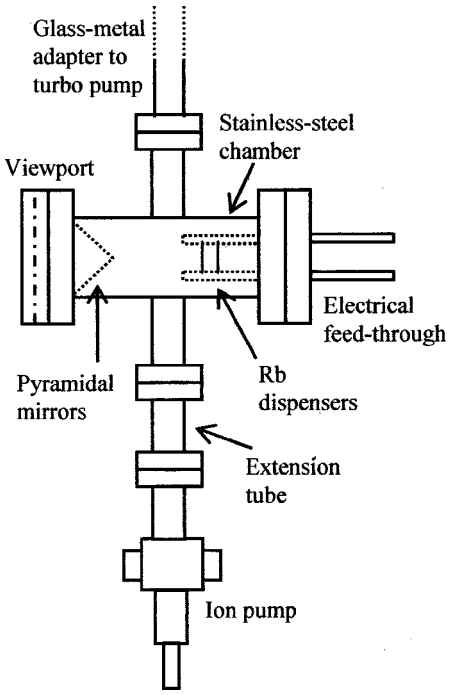

Fig. 4. Schematic of the vacuum layout.

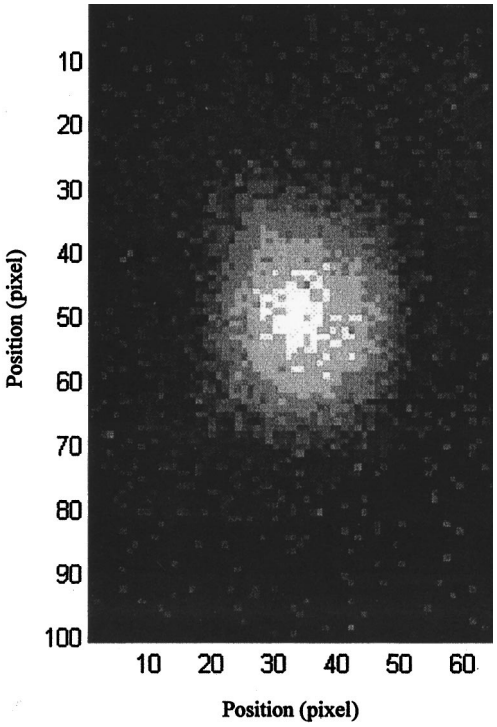

Fig. 5. Typical image of a laser cooled atomic cloud. Pixel size is 12.8 μm.

V. MAGNETIC FIELDS

The magnetic field gradient required to form the MOT is produced by a pair of coils in an anti-Helmholtz configuration. Each coil is 38 mm in diameter and has 16 turns of 0.8-mm-diam insulated copper wire. The coils are spaced 19 mm apart and connected so that the current circulates through each in opposing directions. A current of 4 A produces a suitable gradient of 10 G/cm. The coils are wound directly onto the outside of the tubular vacuum chamber and positioned so that the magnetic field zero is located at the center of the hollow pyramidal region. Small Teflon™ plastic rings that clip around the outside of the chamber are used to hold the wire in place while the coils are wound: the coils are then set in place using a small amount of epoxy.

Although the ion pump is attached to the chamber in an orientation which minimizes the stray field its magnet produces at the MOT, its 4.5-G field is still the dominant background magnetic field. This is not sufficient to stop the MOT from working, but it does cause a 4.5-mm displacement of the trapped sample from the center of the light beams. Rather than moving the anti-Helmholtz coils with an $x-y$ translator as was done by Lee *et al.*,[15] we correct this displacement using three coils (100 mm diameter, 70 turns, requiring approximately 1-A dc current) oriented along orthogonal axes. Standard MOT setups often use three pairs of Helmholtz coils to remove the background magnetic field, but these are ineffective at dealing with any field gradient and often limit optical access to the MOT.

VI. OPERATION OF THE TRAP AND MEASUREMENTS

To observe laser cooling and trapping of atoms we use a low-cost charge coupled device (CCD) camera as discussed in Ref. 9. For measurement of the cloud shape it is useful to use a zoom lens [16]. Those designed for machine-vision are ideal, e.g., a lens for imaging micro-electronic circuits during assembly. The first time a MOT is formed it is best to view the entire hollow pyramid, since stray magnetic fields can move the trap center almost anywhere between the mirrors. Also, if the rubidium vapor pressure is too high, fluorescence from the background vapor can obscure the cloud of trapped atoms.

MOT operation relies on setting a few simple parameters correctly. The details described above ensure that there is: sufficient laser power, a circularly polarized laser beam that is incident on the pyramid, a magnetic field gradient with zero field centrally located within the hollow pyramid, an appropriate trapping laser detuning, and a low background (nonrubidium) vapor pressure. Remaining parameters to be set are the background rubidium vapor pressure and the orientation of the magnetic field gradient.

The rubidium vapor pressure required for best MOT performance is small enough that fluorescence from the background vapor is difficult to see with the CCD camera. This is easiest to detect when the trapping beam is not filling the entire hollow pyramid region (achieved by removing the $f=20$-mm lens), and the laser is scanning across the full Doppler width of the $5S_{1/2}\rightarrow 5P_{3/2}$ transition. For the particular Rb dispenser we use, Rb is liberated at the specified rate when the current is 5.1 A, but the current required in day-to-day operation of the MOT is less than this. When the rubidium dispenser is first switched on, the Rb adheres to the chamber walls until a layer forms, at which point the vapor pressure increases rapidly. During the first attempt at forming a MOT, we slowly increase the dispenser current, at a rate of 0.2 A every 5 min, starting at 2.5 A, until we observe very weak fluorescence from background vapor. We then look for an atomic cloud at the high vapor pressure by expanding and aligning the trapping beam, frequency locking the lasers, setting the trapping laser detuning, and switching on the magnetic field gradient.

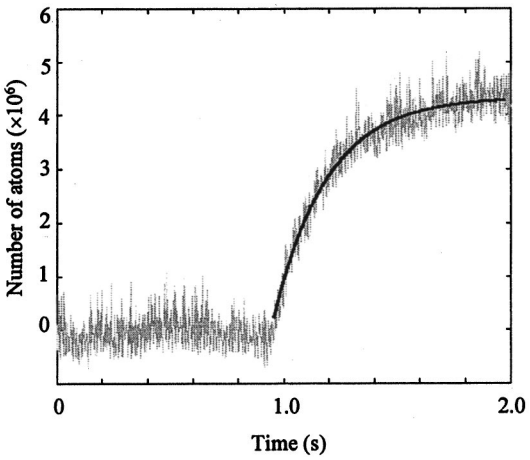

Fig. 6. Number of trapped atoms vs time (for a Rb dispenser current of 3.5 A on for many hours). Dark solid line is the fit to the data.

If a MOT does not form, the most likely reason is that the orientation of the magnetic field gradient is not matched to the circular polarization of the incident trapping beam, and this is corrected by reversing the direction of the current in the anti-Helmholtz coils. At this point a MOT should form. If this does not happen, we check the parameters listed above, starting with the laser frequencies. Once a MOT forms, it is then possible to optimize the dispenser current. After a few days of operation, a current of approximately 3.5 A produces enough Rb for good MOT operation.

Using expressions given in Ref. 9, and following the authors' suggestion of a low-cost large-area photodiode detector, it is possible to measure the number of trapped atoms. We use a large area photodiode-based laser power meter [17] and therefore avoid the problem of calibrating the response of the photodiode. With 1.3 mW/cm^2 of trapping laser intensity we obtain approximately 4×10^6 ^{87}Rb atoms. The number of atoms is limited by our choice of a small (low-cost and compact) vacuum chamber which limits the beam size, the low power available from a simple ECDL, and the scattering of light from pyramidal mirror imperfections. Without quantifying the effect of light scattering, or determining the vapor pressure and effective trapping volume, a quantitative comparison with other pyramidal MOT setups is difficult. However, Lee *et al.* report 1.2×10^7 ^{85}Rb atoms using a 2.1-cm-diam trapping beam, with an intensity of 1.9 mW/cm^2, and a pyramid with a 1.7-cm square base.[15]

Figure 5 shows a typical image of a laser cooled sample of 3.4×10^6 atoms. By calibrating the magnification of the imaging system, it is possible to determine the cloud size and therefore the density. A Gaussian fit to the shape of the cloud gives a cloud size (1/*e* diameter) of 0.45 mm. The typical growth rate of the trapped sample, as measured with the photodiode power meter after rapid switch on of the field gradient, is shown in Fig. 6. The time constant τ for this growth, obtained by fitting to the expression[9] $N(t)=N_0(1-e^{t/\tau})$, is 0.23 s.

Although the above measurements are typical of standard laser cooling and trapping setups, there are some features of the pyramidal MOT which are specific to this type of trap. Since the atoms are trapped close to the mirror, the alignment of the trapping beam with respect to the pyramid, and its collimation, are not at all critical. We can misalign the incident trapping beam by as much as 23° away from the axis of the pyramidal mirror before atoms are no longer trapped. This means that the 90° angle between opposing mirrors forming the pyramid is not at all critical. However, the proximity of the trap center to the mirror surfaces means that light scattered from imperfect joints between the mirrors and from imperfections on the mirror surfaces can be a problem for two reasons. First, the scattered light can cause trap loss. We find that if the cloud of trapped atoms is positioned on the central axis of the pyramid (using the bias coils) its shape becomes severely distorted and atoms are lost due to the intensity imbalance associated with the poor quality reflection of the trapping light at the joints between the mirrors. Second, the intensity of the scattered light can be substantially greater than the fluorescence from the cloud, so that subtracting this background (critical to making an accurate measurement of the number of trapped atoms) is more critical. Because the silver mirrors cannot be cleaned as easily as a glass cell window, the background noise from unwanted light scattering is worse in a pyramidal MOT of the sort we describe than in the standard MOT described in Ref. 9. However, the simplicity of the pyramidal MOT makes it ideally suited to an undergraduate laboratory environment.

ACKNOWLEDGMENTS

We gratefully acknowledge the financial support of the Royal Society of New Zealand Marsden Fund (Contract No. UOO910) and the University of Otago. We also thank Nick Thomas for his advice on practical matters.

APPENDIX: COMPONENTS USED IN PYRAMIDAL TRAP CONSTRUCTION

The following list includes the commercial components we used to construct the apparatus, with the exception of the ECDLs and certain common items which are identical to those listed in Ref. 9. Suppliers and part numbers are given to enable the reader to determine component specifications, and the prices given are indicative only. Components from other manufacturers may well be cheaper and equally suitable, or even perform better. No endorsement by the University of Otago is implied. Items in the Appendix are listed in brackets throughout this paper.

[1] Mixer, part ZAD 8 $55, Mini-Circuits, 13 Neptune Avenue, Brooklyn, NY 11235; www.minicircuits.com.

[2] Optical breadboard, 60 cm×60 cm, part T11312 $680, Thorlabs, 435 Route 206, P.O. Box 366, Newton, NJ 07860; www.thorlabs.com.

[3] Quarter-wave plates, part WPMQ05M-780 $266, Thorlabs, 435 Route 206, P.O. Box 366, Newton, NJ 07860; www.thorlabs.com.

[4] Lenses: part LA1074-B ($f=20$ mm) $27 each; part LA1380-B ($f=500$ mm) $36; cylindrical lens, part LJ1810L2-B ($f=25$ mm) $63; Thorlabs, 435 Route 206, P.O. Box 366, Newton, NJ 07806; www.thorlabs.com.

[5] Anamorphic prism pair, part 420-1212-830 $90, Optima Precision, 775 SW Long Farm Road, West Linn, OR 97068; www.optima-prec.com.

[6] Although we construct our own pyramid mirrors, a variety of optical companies can provide this service. See (for example) those listed in the annual *Physics Today* buyers

guide. For related items we have used Comar Instruments, 70 Hartington Grove, Cambridge CB1 4UB, England; phone: +44 1223 245470.

[7] Torr Seal low vapor pressure epoxy, part 953-0001 $60, Varian Vacuum Products, 121 Hartwell Avenue, Lexington, MA 02421; www.varianinc.com/vacuum.

[8] Reducing four-way cross, Ref. 150-4-075 (part 405011) $170, MDC Vacuum Products, 23842 Cabot Blvd., Hayward, CA 94545-1651; www.mdc-vacuum.com.

[9] Ion pump, part 9190520 $485, Alnico magnet 9190038 $185, Minivac controller (120 VAC) 9290190 $990, Varian Vacuum Products, 121 Hartwell Avenue, Lexington, MA 02421; www.varianinc.com/vacuum.

[10] Extension tube, part PF 520 201-X $65, Pfeiffer Vacuum Technology, 24 Trafalgar Square, Nashua, NH 03063-1988; www.pfeiffer-vacuum.com.

[11] High current feedthrough, part PF 671 011-X (UMD 440) $310, Pfeiffer Vacuum Technology, 24 Trafalgar Square, Nashua, NH 03063-1988; www.pfeiffer-vacuum.com.

[12] Rubidium (alkali) metal dispenser, part RB/NF/3.4/12 FT10+10 (10 dispensers) $110, SAES Getters, 1122 East Cheyenne Mountain Blvd., Colorado Springs, CO 80906; www.saesgetters.com.

[13] Glass to metal adaptor, Ref. GA-050P-S (part 460005) $50, MDC Vacuum Products, 23842 Cabot Blvd., Hayward, CA 94545-1651; www.mdc-vacuum.com.

[14] Viewport, Ref. VP 150 (part 450002) $105, MDC Vacuum Products, 23842 Cabot Blvd., Hayward, CA 94545-1651; www.mdc-vacuum.com.

[15] Acetone (AnalaR quality), part 100034Q 2.5L $20, BDH Laboratory Supplies, Poole BH15 1TD, England, www.bdh.com.

[16] Zoom lens, see Edmund Industrial Optics, 101 East Gloucester Pike, Barrington, NJ; www.edmundoptics.com.

[17] Power meter, part S120 $872, Thorlabs, 435 Route 206, P.O. Box 366, Newton, NJ 07860; phone: +1 973 579 7227; www.thorlabs.com.

[1]Sarah L. Gilbert and Carl E. Wieman, "Laser cooling and trapping for the masses," Opt. Photonics News **4** (7), 8–14 (1993).

[2]M. H. Anderson, J. R. Ensher, M. R. Matthews, C. E. Wieman, and E. A. Cornell, "Observation of Bose–Einstein condensation in a dilute atomic vapor," Science **269**, 198–201 (1995); Isaac F. Silvera, "Bose–Einstein condensation," Am. J. Phys. **65** (6), 570–574 (1997).

[3]M.-O. Mewes, M. R. Andrews, D. M. Kurn, D. S. Durfee, C. G. Townsend, and W. Ketterle, "Output Coupler for Bose–Einstein Condensed Atoms," Phys. Rev. Lett. **78** (4), 582–585 (1997); Daniel Kleppner, "A beginner's guide to the atom laser," Phys. Today 11–13 (August, 1997).

[4]*Proceedings of the International School of Physics "Enrico Fermi," Course CXVIII, Laser Manipulation of Atoms and Ions*, edited by E. Arimondo, W. D. Phillips, and F. Strumia (North-Holland, Amsterdam, 1992).

[5]The 1997 Physics Nobel Prize was awarded to Steven Chu, Claude Cohen-Tannoudji, and William D. Phillips, for development of methods to cool and trap atoms with laser light. The 2001 Physics Nobel Prize was awarded to Eric Cornell, Carl Wieman, and Wolfgang Ketterle, for the achievement of Bose–Einstein condensation in dilute gases of alkali atoms, and for early fundamental studies of the properties of the condensates.

[6]M. R. Anderson, C. G. Townsend, H.-J. Miesner, D. S. Durfee, D. M. Kurn, and W. Ketterle, "Observation of interference between two Bose condensates," Science **275**, 637–641 (1997).

[7]L. Deng, E. W. Hagley, J. Wen, M. Trippenbach, Y. Band, P. S. Julienne, J. E. Simsarian, K. Helmerson, S. L. Rolston, and W. D. Phillips, "Four-wave mixing with matter waves," Nature (London) **398**, 218–220 (1999).

[8]Elizabeth A. Donley, Neil R. Claussen, Simon L. Cornish, Jacob L. Roberts, Eric A. Cornell, and Carl E. Wieman, "Dynamics of collapsing and exploding Bose-Einstein condensates," eprint cond-mat/0105019 2001.

[9]Carl Wieman, Gwenn Flowers, and Sarah Gilbert, "Inexpensive laser cooling and trapping experiment for undergraduate laboratories," Am. J. Phys. **63** (4), 317–330 (1995).

[10]K. B. MacAdam, A. Steinbach, and C. Wieman, "A narrow-band tunable diode laser system with grating feedback and a saturated absorption spectrometer for Cs and Rb," Am. J. Phys. **60** (12), 1098–1111 (1992).

[11]Paul Feng and Thad Walker, "Inexpensive diode laser microwave modulation for atom trapping," Am. J. Phys. **63**, 905–908 (1995).

[12]Daryl W. Preston, "Doppler-free saturated absorption: Laser spectroscopy," Am. J. Phys. **64** (11), 1432–1436 (1996).

[13]Phillip Gould, "Laser cooling of atoms to the Doppler limit," Am. J. Phys. **65**(11), 1120–1123 (1997).

[14]Yukiko Shimizu and Hiroyuki Sasada, "Mechanical force in laser cooling and trapping," Am. J. Phys. **66** (11), 960–967 (1998).

[15]K. I. Lee, J. A. Kim, H. R. Noh, and W. Jhe, "Single-beam atom trap in a pyramidal and conical hollow mirror," Opt. Lett. **21** (15), 1177–1179 (1996); J. A. Kim, K. I. Lee, H. R. Noh, and W. Jhe, "Atom trap in an axicon mirror," *ibid.* **21** (2), 117–119 (1997).

[16]J. J. Arlt, O. Maragò, S. Webster, S. Hopkins, and C. J. Foot, "A pyramidal magneto-optical trap as a source of slow atoms," Opt. Commun. **157**, 303–309 (1998).

[17]R. S. Williamson III, P. A. Voytas, R. T. Newell, and T. Walker, "A magneto-optical trap loaded from a pyramidal funnel," Opt. Express **3** (3), 111–117 (1998).

[18]A. S. Arnold, J. S. Wilson, and M. G. Boshier, "A simple extended-cavity diode laser," Rev. Sci. Instrum. **69** (3), 1236–1239 (1998). We use this ECDL design with a Sanyo DL-7140-201 laser diode.

[19]L. Ricci, M. Weidemüller, T. Esslinger, A. Hemmerich, C. Zimmermann, V. Vuletic, W. König, and T. W. Hänsch, "A compact grating stabilized diode laser for atomic physics," Opt. Commun. **117**, 541–549 (1995).

[20]G. D. Rovera, G. Santarelli, and A. Clairon, "A laser diode system stabilized on the cesium D_2 line," Rev. Sci. Instrum. **65**(5), 1502–1505 (1994).

[21]K. G. Libbrecht and J. L. Hall, "A low-noise high speed diode laser current controller," Rev. Sci. Instrum. **64** (8), 2133–2135 (1993).

[22]Using the following procedures with Conflat-type flanges we have never had a leak. Make sure the flange knife edges are clean (use acetone, a hemostat, and an optical tissue to wipe clean if necessary); always use a new copper gasket; make sure the gasket is positioned correctly between the two faces of the flange; tighten each of the bolts by hand and check that the gap between the two faces of the flange is even around the entire circumference; tighten opposing pairs of bolts with a torque wrench in small steps; keep tightening until the two faces of the flange meet squarely.

[23]Nigel S. Harris, *Modern Vacuum Practice* (McGraw–Hill, London, 1989).

A Universal Serial Bus interface for electronics projects and instruments

T. Z. Fullem and C. D. Spencer[a)]
Department of Physics, Ithaca College, Ithaca, New York 14850

(Received 30 July 2001; accepted 18 March 2002)

[DOI: 10.1119/1.1477436]

I. INTRODUCTION

The Universal Serial Bus (USB) has become a standard interface between computers and their peripherals. This note describes a commercial USB device that can be used as a 16-bit parallel input/output port for interfacing personal computers to physics laboratory experiments. After describing the device, we illustrate how it can be used as a multiscaler and how the multiscaler can be used in a photogate experiment.

II. THE ACTIVEWIRE USB PARALLEL PORT: HARDWARE AND SOFTWARE

An inexpensive ($59), credit-card sized ActiveWire™ USB board is shown in Fig. 1.[1] The USB plug is in the foreground and two twenty-pin headers for connections to application circuits are on the back. The board is powered by the computer through +5 V and ground connections in the USB cable. Specifications, manuals, software drivers, and sample programs can be downloaded from ActiveWire's web site.[1]

For our applications, we need only the ground and $I/O_0 \cdots I/O_{15}$ connections from the USB board. We use five of the Visual Basic subroutines supplied by the manufacturer. The routines open and close the port, select which I/O connections perform inputs and which perform outputs, and carry out input and output operations. In the following descriptions, Visual Basic variable names are in a courier font, for example, `AWusb` stands for ActiveWire USB.

The subroutine `AWusbOpen 0` opens board 0 for operations. The first board connected to a USB plug is assigned device number 0 by the computer while additional boards are assigned, in the order connected, 1, 2, etc. Only one board may be open at a time. The subroutine `AWusbClose` deactivates the current open board.

The subroutine call `AWusbEnablePort value, 2` selects which connections of the current open board are inputs and which are outputs. We specify `value` as a 16-bit hexadecimal number with each high binary bit selecting the corresponding I/O connection as an output and each low bit selecting the corresponding connection as an input. The 2 specifies the number of bytes of `value` (and is always 2 in this subroutine). For example, the subroutine call `AWusbEnablePort &HFFFF, 2` selects all 16 connections as outputs; while the call `AWusbEnablePort 0, 2` makes all 16 connections inputs.

The call `AWusbInPort data, 2` returns with `data` equal to the binary value of the input connections at the instant the call is made. A low bit in `data` means the corresponding I/O connection is programmed for input and the connection was low. A high bit in `data` means the corresponding I/O connection is programmed for input and the connection was high. (The corresponding bit in `data` for an I/O connection programmed for output is high.)

The subroutine call `AWusbOutPort data, 2` puts the low 16 bits of the binary value of `data` on the I/O connections. Specifically, the output operation makes each connection that is programmed as an output equal to the corresponding bit of `data`. Output values are maintained on the connections until changed by calling `AWusbOutPort data, 2` with a different `data` value. (Connections programmed for input are not affected by outputs.)

III. EXAMPLE APPLICATION

To illustrate the use of the USB board, we present an application which repeatedly counts and makes available to the computer the number of events in a succession of control intervals. The application is carried out by the circuit in Fig. 2 and the program in Fig. 3.

The circuit consists of three cascaded counters, an AND gate, two input signals (events and control), and the USB interface. The counters count low-to-high transitions of the AND output when CLEAR is low. The counters are zero when CLEAR is high. When control is low, the AND output is low and the counters do not count. When control is high, the AND output is the same as events and the counters count low-to-high transitions of the events signal (if CLEAR is low).

The low 13 USB board connections are enabled as inputs and the high three connections are enabled as outputs. The counter outputs go to connections 0 through 11. The control signal goes to input connection 12 so that the program can determine when the counters are counting and when they are stopped. Finally, output connection 15 goes to each counter's CLEAR input. The program can set the counters to zero by making connection 15 high and the program can enable counting by making connection 15 low.

The Visual Basic program in Fig. 3 supposes a succession of high control signal pulses which may begin before or after program initiation. Further, the control signal may be either high or low at program initiation.

The first three program operations: (1) open the ActiveWire USB as device 0; (2) enable the high three connec-

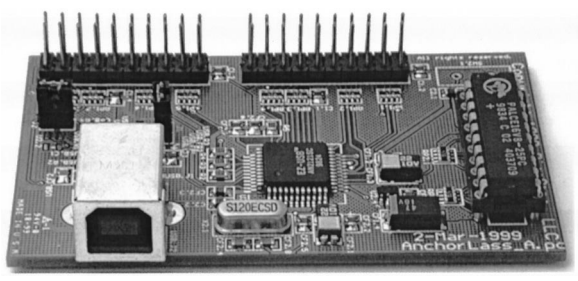

Fig. 1. Photograph of the ActiveWire USB parallel port board.

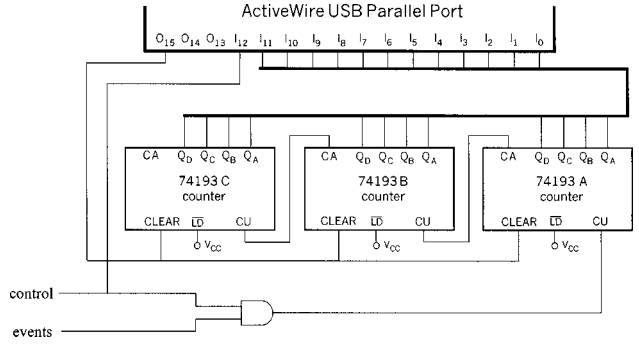

Fig. 2. Multiscalar circuit connected to the ActiveWire USB parallel port. The counters count low-to-high transitions of the events signal when the control signal is high and CLEAR is low.

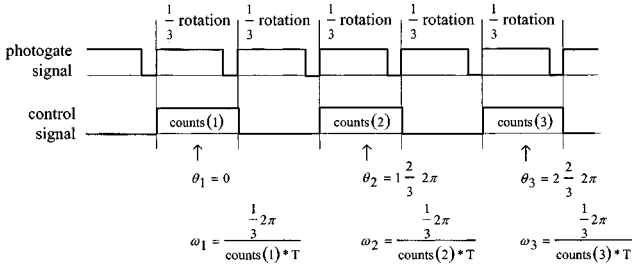

Fig. 4. Photogate signal produced by a rotating pulley with three evenly spaced holes in its side. The signal is low when light passes through a hole. The control signal is produced by toggeling the photogate signal. Because control is high for 1/3 of a revolution every other 1/3 of a rotation, ω vs θ can be computed. T is the known period of the digital clock connected to the events signal (in Fig. 2).

tions to be outputs and the remaining connections to be inputs; and (3) set output connection 15 high, thus set the counters to zero.

While the counters are held at zero, the next seven lines of program code synchronize the program with the control signal. The goal of the code is to end when control has definitely gone from high to low. If control is initially low, the program waits for low to end and then for high to end before being synchronized. If control is initially high, the program immediately exits the first `Do While` loop and then waits for high to end. (Synchronization is not needed when control is initially low and only goes high with the first count interval after the program starts.)

The `For` loop determines the number of events that occur during a high control interval. The number of loop repetitions is the value of `no_inputs` (a Visual Basic text box). The first output makes all connections which are programmed for output low and thus makes CLEAR low. The counters (previously set to zero) start counting when control goes high. When control returns low, the input connections are read and the count (low twelve bits) is stored in an array. The counters are then reset to zero by making CLEAR high and the loop repeats. For the `For` loop to end, the number of high control pulses after program initiation must be greater than the value of `no_inputs`.

The last operation (after the `For` loop) closes the USB port. After acquisition is complete, the data array `counts(i)` may be manipulated, displayed, plotted, and saved.

```
AwusbOpen 0                          ' open Active Wire USB as device 0
AwusbEnablePort &HE000, 2            ' make high 3 bits outputs, rest inputs
AwusbOutPort &H8000, 2               ' make out bit 15 high which zeros counters

AwusbInPort data, 2                  ' synchronize by waiting for the end of first
Do While (data And 2 ^ 12) = 0       '    high control interval
   AwusbInPort data, 2
Loop
Do While (data And 2 ^ 12) = 2 ^ 12
   AwusbInPort data, 2
Loop

For i = 1 To no_inputs
   AwusbOutPort 0, 2                  ' make out bit 15 low which enables counters
   AwusbInPort data, 2                ' wait until control at input bit 12 goes
   Do While (data And 2 ^ 12) = 0     '    goes high
      AwusbInPort data, 2
   Loop
   Do While (data And 2 ^ 12) = 2 ^ 12   ' wait until control returns low
      AwusbInPort data, 2
   Loop
   AwusbInPort data, 2                ' input count data
   counts(i) = data And &HFFF         ' extract lower 12 bits which is the count
   AwusbOutPort &H8000, 2             ' make out bit 15 high which zeroes counters
Next i

AwusbClose                           ' close Active Wire USB
```

Fig. 3. Visual Basic data collection program used with the circuit in Fig. 2. The code sets up the USB port, sets the counters to zero, synchronizes with control, reads the count values for `no_inputs` high control intervals, and closes the port.

IV. EXAMPLE EXPERIMENT

To illustrate the system's capability, we used a photogate and flip-flop, the circuit in Fig. 2 and the program in Fig. 3 to measure the acceleration of a falling mass that is attached to string wound on a freely rotating pulley.[2] The pulley has three holes in its side. During one revolution, the holes unblock light from a photogate three times creating the timing pattern shown in Fig. 4. (We wire our phototransistors to produce a high digital signal when light is blocked and a low signal when the transistor is turned on by light.[2]) The photogate output is used to toggle a flip-flop to produce the control signal for the circuit. Control is high for 1/3 of a revolution every other 1/3 of a revolution. The events signal is a digital clock of known frequency in the range of 25–50 kHz.

Data are collected by starting the program in Fig. 3 and then releasing the falling mass. The synchronization steps in the program allow for the control signal to be initially either high or low. We arrange our system so the string releases from the pulley when the mass reaches the floor and the pulley keeps spinning with minimal deceleration. Thus, the value of `no_inputs` is not critical.

Using a digital clock of known period for control, and a higher frequency clock for events, we obtain the expected count values (with an accuracy of ± 1) provided the high control pulses are at least 8 ms long and the low intervals between high pulses are also at least 8 ms. We found that these minimum times are a property of the USB and the ActiveWire board, not the host computer's speed.

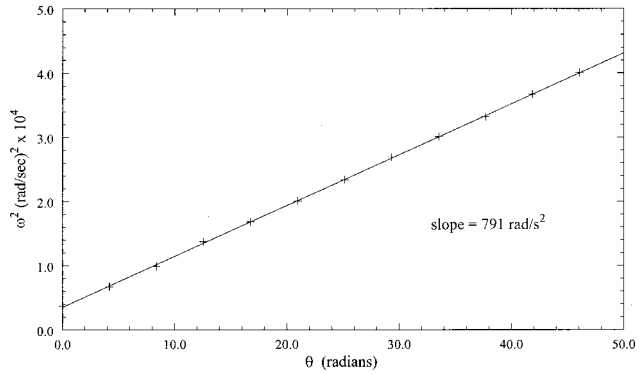

Fig. 5. Plot of ω^2 versus θ pulley data taken with the timing in Fig. 4, the circuit of Fig. 2, and the program of Fig. 3. The data should lie along a straight line of slope 2α.

After collecting data, the `counts(i)` array is observed and only values recorded while the system was accelerating are kept. Then, `counts(i)` multiplied by the clock period (T) equals the duration of the ith 1/3 of a revolution. Thus, ω versus θ can be calculated as shown in Fig. 4. Assuming the angular acceleration of the system is constant, a plot of ω^2 versus θ should be a straight line of slope $2\alpha = 2a/r$ where r is the radius of the pulley and a is the linear acceleration of the system. Results from a falling mass of 40 g are given in Fig. 5. The expected straight line is found; with $r = 2.34$ cm, the value of a from the slope is 925 cm/s^2, which is consistent with results from running the experiment using other interfaces.[2]

V. CONCLUSIONS

In addition to the pulley experiment described above, we have used the USB board with other photogate experiments. We have also used it to perform half-life and statistics[3] experiments where the control signal is a clock and the events signal is digitized pulses from radioactive decay. Further, we have used the USB board to implement handshaking[4] and non-handshaking[5] voltage loggers as well as a crude pulse height analyzer.[6] We have also used the board to control an 8254 programmable interval timer.[7] We have found that the ActiveWire USB interface is a convenient and reliable interface suitable for many applications.

ACKNOWLEDGMENT

The work described here was supported by the Clinton Ford Science Research Fund of Ithaca College.

[a]Electronic mail: spencer@ithaca.edu

[1]For availability, specifications, manuals, and software, see www.activewireinc.com. ActiveWire is a registered trademark of PicoStar, LLC.

[2]C. D. Spencer and P. F. Seligmann, "An Independent Freshman Laboratory," Phys. Teach. **30**, 310–314 (1992).

[3]D. A. Briotta, P. F. Seligmann, P. A. Smith, and C. D. Spencer, "The appropriate use of microcomputers in undergraduate physics labs," Am. J. Phys. **55**, 891–897 (1987).

[4]C. D. Spencer, "A capable voltage logger for the PCI bus," Am. J. Phys. **68**, 966–968 (2000).

[5]C. D. Spencer, *Digital Design for Computer Data Acquisition* (Cambridge U.P., Cambridge, 1990), pp. 85–99.

[6]We will provide upon request a circuit diagram and program listing for the PHA.

[7]Reference 5, pp. 129–161.

PHYSICS AND POETRY

It was not only the content of her papers that brought down on her such lofty contempt, but her style of expression. More than one of the assigned readers had commented that she did not write like a physicist, and, oddly, hadn't intended their remarks as praise. She still holds fast to the doctrine her father had instilled in her, that the very best physics is very good poetry, so that when she can, she always chooses metaphor over mathematics.

Rebecca Goldstein, *Properties of Light: A Novel of Love, Betrayal, and Quantum Physics* (Houghton Mifflin Company, New York, NY, 2000), p. 143.

Submitted by Alan DeWeerd.